

# Studies of the Structure and Composition of Rhenium–1,1-Hydroxyethylidenediphosphonate (HEDP) Analogues of the Radiotherapeutic Agent $^{186}\text{ReHEDP}$

R. C. Elder,<sup>\*,†</sup> Jie Yuan,<sup>†</sup> Bella Helmer,<sup>†</sup> David Pipes,<sup>‡</sup> Karen Deutsch,<sup>‡</sup> and Edward Deutsch<sup>‡</sup>

Biomedical Chemistry Research Center, Department of Chemistry, University of Cincinnati, Cincinnati, Ohio 45221-0172 and Mallinckrodt Medical Inc., 675 McDonald Boulevard, P.O. Box 5840, St. Louis, Missouri 63134

Received August 14, 1996<sup>⊗</sup>

Complexes of technetium with diphosphonate ligands are widely used for the imaging and diagnosis of bone disease and most especially metastatic bone cancer. Analogous complexes of radioactive rhenium ( $^{186}\text{Re}$ ) with the ligand  $\text{H}_4\text{HEDP}$ , 1,1-hydroxyethylidenediphosphonate, have been shown to be effective palliatives for the treatment of the intense pain associated with metastatic bone cancer. We have synthesized several of these analogs using nonradioactive Re and have structurally characterized them using EXAFS (extended X-ray absorption fine structure) spectroscopy. One complex synthesized via the substitution reaction of HEDP with *trans*- $[(\text{py})_4(\text{O})_2\text{Re}]\text{-Cl}$  in absolute ethanol appears to be the 1:1 salt of the tris-HEDP complex anion with the starting Re cation,  $[(\text{py})_4(\text{O})_2\text{Re}][\text{Re}(\text{H}_2\text{HEDP})_3]$ . Three other materials, all synthesized via reduction of perrhenate by stannous chloride in the presence of excess  $\text{H}_4\text{HEDP}$  ligand, are quite different in structure from the material formed by substitution. The principal difference is that each of these contains Re–Re bonds and is formulated as oligomers. The material with a large excess of reductant has Re–Re bonds of ca. 2.4 Å and is best modeled as a linear tetramer of rhenium atoms bridged by HEDP ligands which also bind an equivalent number of tin atoms with additional HEDP ligands. It is formulated as  $\text{Li}_x[\text{Re}_4(\text{OH})_2\text{Sn}_4(\text{HEDP})_{12}]$ . The material formed with the least amount of reducing agent is best modeled as a triangular cluster of rhenium atoms biccapped by two HEDP ligands and bridged to three tin atoms by HEDP to form a complex  $\text{Li}_x[\text{Re}_3\text{Sn}_3(\text{HEDP})_8]$ . It also has Re–Re bonds but of a significantly longer distance, ca. 2.8 Å. A material with an intermediate amount of reducing agent, prepared in a manner most closely resembling the medically effective palliative agent, appears to contain a mixture of these, and perhaps other, oligomers.

## Introduction

Two of the most common and deadliest diseases are prostate cancer in men and breast cancer in women. Both types of cancers often result in widespread metastases to the skeleton, and despite conventional treatments (surgical, hormonal, external radiation, chemotherapy, etc.) these patients often experience severe and debilitating skeletal pain. For more than 50% of these patients, pain cannot be adequately controlled despite the liberal use of narcotics, high doses of nonsteroidal antiinflammatory drugs (NSAIDs), or acetaminophen.

In order to better control the intense pain associated with metastatic bone cancer, we have developed the bone-seeking radiotherapeutic agent  $^{186}\text{ReHEDP}$ , where HEDP represents 1,1-hydroxyethylidenediphosphonate.<sup>1–3</sup> This radiopharmaceutical is based, first, on the observation that skeletal pain can be relieved by delivering a therapeutic dose of  $\beta$  radiation to the metastatic site, second, on the well known bone-seeking abilities of the diagnostic  $^{99\text{m}}\text{Tc}$  diphosphonate radiopharmaceuticals, and third, on the periodic relationship between technetium and rhenium.<sup>4,5</sup>

Despite extensive studies of the synthesis, HPLC behavior, and composition of the  $^{99\text{m}}\text{Tc}$  diphosphonates (and their  $^{99\text{g}}\text{Tc}$  analogues), very little is actually known about the formulation and structure of these medically important agents.<sup>6–8</sup> Even less is known about the formulation and structure of the  $^{186}\text{Re}$  diphosphonates, largely because these substances are not sufficiently stable to allow analytical HPLC separations,<sup>9</sup> nor have we been able to grow suitable single crystals for an X-ray structure determination. All the studies to date, and all the experimental data currently in hand, do support the description of Tc/Re diphosphonates as relatively labile mixtures of oligomeric or polymeric complexes. However, these studies and data do not cast any light at all on the possible role of tin (used as a reductant to generate the Tc/Re diphosphonates) in these mixtures, nor do they provide any firm structural data. The studies described in this paper are designed to amplify our current state of knowledge of the structures of the prototypical rhenium diphosphonate, ReHEDP. Some of our initial EXAFS observations on ReHEDP have been previously reported in meeting abstracts.<sup>10–12</sup>

\* Author to whom correspondence should be addressed.

<sup>†</sup> University of Cincinnati

<sup>‡</sup> Mallinckrodt Medical Inc.

<sup>⊗</sup> Abstract published in *Advance ACS Abstracts*, June 1, 1997.

- (1) Maxon, H. R.; Deutsch, E. A.; Thomas, S. R.; Libson, K.; Lukes, S. J.; Williams, C. C.; Ali, S. *Radiology* **1988**, *166*, 501.
- (2) Maxon, H. R.; Thomas, S. R.; Hirtzberg, V. S.; Schroder, L. E.; Englaro, E. E.; Samaratunga, R.; Scher, H. I.; Moulton, J. S.; Deutsch, E. A.; Deutsch, K. F.; Schneider, H. J.; Williams, C. C.; Erhardt, G. *J. Semin. Nucl. Med.* **1992**, *22*, 33.
- (3) Pipes, D. W.; Deutsch, E. *Drugs Future* **1993**, *18*, 520.

- (4) Volkert, W. A.; Deutsch, E. A. *Advances in Metals in Medicine*; JAI Press Inc.: Greenwich, CT, 1993; Vol. 1, pp 115–153.
- (5) Deutsch, E.; Libson, K.; Vanderheyden, J.-L. *Technetium and Rhenium in Chemistry and Nuclear Medicine 3*; Raven Press: New York, 1990; pp 13–22.
- (6) Libson, K.; Heineman, W. R.; Deutsch, E. *Med. Nucl. Informacao* **1986**, *3*, 35.
- (7) Zodda, J. P.; Tanaba, S.; Heineman, W. R.; Deutsch, E. *Appl. Radiat. Isot.* **1986**, *37*, 345.
- (8) Martin, J. L. Jr.; Yuan, J.; Lunte, C. E.; Elder, R. C.; Heineman, W. R.; Deutsch, E. *Inorg. Chem.* **1989**, *28*, 2899.
- (9) Pipes, D.; Miller, K.; Wolfangel, R.; Pilcher, G.; Deutsch, E. *J. Nucl. Med.* **1990**, *31*, 768a.

## Experimental Section

**Reagents.** These were obtained as follows: 1,1-hydroxyethylidenediphosphonate, disodium salt ( $\text{Na}_2\text{H}_2\text{HEDP}$ ) from Mallinckrodt Medical Inc., 1,1-hydroxyethylidenediphosphonic acid ( $\text{H}_4\text{HEDP}$ ) from Fluka Chemical Co., stannous chloride dihydrate from Mallinckrodt Chemical Co., gentisic acid (2,5-dihydroxybenzoic acid), stannous chloride anhydrous, sodium perrenate (99.9%) and potassium perrenate (99.9%) from Aldrich Chemical Co., DEAE anion exchange resin from Whatman Co. was pretreated before use as described in the package insert.  $\text{trans}-(\text{py})_4(\text{O})_2\text{ReCl}$  was prepared by literature methods.<sup>13</sup>  $\text{Sn(IV)HEDP}$  was prepared by dissolving  $\text{Na}_2\text{H}_2\text{HEDP}$  (0.20 g) in 5 mL water in a small test tube. Stannous chloride dihydrate (0.080 g) was dissolved in the solution and air was bubbled through for 6 h. An oily residue formed which was redissolved in 5 mL of water. The pH was adjusted to 5.5 with 1 M NaOH (aqueous) and placed in a drying oven set at 95 °C. The sample was dried overnight, resulting in a white, semicrystalline solid. A small sample was dissolved in water and titrated with iodine using a starch indicator. No evidence of stannous ion was found. All other chemicals were of reagent grade. Barnstead distilled/deionized water was used to prepare all solutions.

**"High Tin" (H-Sn) ReHEDP Preparation.**  $\text{H}_4\text{HEDP}$  (3.1 g) was dissolved in 35 mL of water in a 100 mL round bottom flask. Sodium perrenate ( $\text{NaReO}_4$ , 0.41 g) was dissolved in this mixture, and an additional 30 mL of water added. The solution was purged with nitrogen gas for 15 min. Anhydrous stannous chloride ( $\text{SnCl}_2$ , 1.38 g) was added with rapid stirring. A condenser was placed on the flask and the solution refluxed under a positive nitrogen pressure for 1 h. The solution changed from colorless to dark brown on heating. This brown solution was cooled and diluted with 300 mL of nitrogen purged water. The reaction solution was loaded onto a DEAE anion exchange resin column (5.0 by 1.5 in.) The column was rinsed with 200 mL of 0.1 M HCl and 400 mL of 0.25 M aqueous LiCl. The dark brown band was then eluted from the column with 200 mL of 1.0 M LiCl. The main portion of the band was collected in a volume of 60 mL. This purified ReHEDP (H-Sn) solution was added slowly to 300 mL of absolute ethanol with rapid stirring. A greenish-brown solid formed after several minutes. The solid was collected by filtration, rinsed with 5 mL of absolute ethanol, and dried under vacuum. Yield 1.415 g. Anal. C, 6.80; H, 3.51; P, 9.27; Re, 10.22; Sn, 7.59; Li, 2.10.

**"Low Tin" (L-Sn) ReHEDP Preparation.** The low tin reduction was the same as that for ReHEDP (H-Sn), except only 0.55 g of anhydrous stannous chloride was used. Yield 0.94 g. Anal. C, 7.51; H, 3.55; P, 13.08; Re, 13.64; Sn, 9.03; Li, 2.44.

**"Clinical" (Clin) ReHEDP Preparation.** The so-called clinical solution was synthesized as follows: A solution of  $\text{KReO}_4$  (1.55 mg/mL) was purged with nitrogen for 15 min. This solution (1.0 mL) was added by syringe to a lyophilized vial containing 10 mg of  $\text{Na}_2\text{H}_2\text{HEDP}$ , 3.5 mg of stannous chloride dihydrate, and 3.0 mg of gentisic acid formulated at pH 2.0. The vial was heated in a laboratory autoclave for 15 min at 121 °C. The concentration of reagents in this preparation is in the same proportions as those used for clinical trials. The concentrations here are less than a ten-fold increase over those actually used in the clinical preparations. The increase in concentration was chosen to allow measurement of acceptable quality EXAFS data.

**"Substitution Prepared" (Subs) ReHEDP Preparation.** The material was synthesized via HEDP substitution onto  $\text{trans}-(\text{py})_4(\text{O})_2\text{ReCl}$  (0.50 g). The Re(V) starting material was dissolved in 10 mL argon purged absolute ethanol in a 50 mL round bottom flask.  $\text{H}_4\text{HEDP}$  (0.84 g) in 1 mL of absolute ethanol was added and the solution refluxed under positive pressure of argon for 3 h. A brown solid formed during heating which was collected by filtration and washed with  $3 \times 4$  mL aliquots of ethanol. Yield 0.89 g. Anal. C, 25.07; H, 3.64; N, 4.54; P, 14.71; Re, 19.05; Cl, <0.11.

**Raman Spectra.** All spectra were measured on a Bio-Rad FT Raman spectrophotometer (FTS-60A) with Nd-YAG laser excitation

(1064 nm). Spectrometer resolution was set for  $2 \text{ cm}^{-1}$  with each resultant spectrum the average of 1024 scans. Samples were prepared and sealed in capillary tubes in an argon atmosphere glove box. Spectra were recorded both on aqueous solutions and solids diluted with finely powdered KBr.

Spectral measurements were attempted for the ReHEDP samples as well as  $\text{trans}-(\text{py})_4(\text{O})_2\text{ReCl}$ , the starting material for preparing (Subs) ReHEDP, and also  $[\text{Ph}_4\text{As}][\text{ReO}(\text{DBDS})]$ , where DBDS is  $N,N'$ -bis-(mercaptoacetyl)butane-1,4-diamine, which provides an example of a five-coordinate rhenium complex with a single "yl" oxygen ligand.<sup>14</sup> Attempts to obtain spectra of ReHEDP (H-Sn, L-Sn, and Clin) were unsuccessful. Either the sample was charred by the exciting laser or the specimens were so dilute that no signal was observable above the noise. The Raman spectrum of (Subs) ReHEDP was obtained successfully.

**EXAFS Data Collection.** To prevent oxidation, samples were kept in argon purged septum vials during storage ( $-15 \text{ }^\circ\text{C}$ ) and transportation. Manipulations were performed in a dry glovebox filled with either argon or nitrogen gas. The amount of sample used was calculated to achieve an overall absorbance change,  $\Delta\chi$ , of  $<1.0$ .<sup>15</sup> When needed, finely powdered BN (boron nitride) was used as diluent. Sample cells were made of aluminum metal or plastic sheet, 0.8 mm thick. Adhesive Kapton tape (3M) was used as the X-ray window and to seal the cell.

X-ray absorption spectra were measured on two types of solutions. The first type, designated as an aqueous solution, was made by dissolving one of the purified ReHEDP preparations in distilled water. The second, designated as a clinical solution, (Clin) ReHEDP, typically had more than a tenfold molar ratio of ligand to rhenium as well as excess reductant and an antioxidant such as gentisic acid. For low temperature measurements, glycerol was added to the solutions in a 1:3 volume ratio before cooling to prevent formation of ice crystals.

Solution cells were made of Teflon sheet with Kapton tape windows. Two pin holes were drilled from the cell top into the sample cavity for injection and a gas bleed. The cell was purged with nitrogen before solution was injected into the cell. Vacuum grease was used to seal the pin holes after the injection. For low temperature experiments, the cell was mounted on the sample holder of the cryostat and plunged into liquid nitrogen immediately after filling.

X-ray absorption spectra were measured at the Stanford Synchrotron Radiation Laboratory (SSRL) and the Cornell High Energy Synchrotron Source (CHESS). Experimental conditions at SSRL typically had ring currents of 50–100 mA at 3.0 GeV with running conditions dedicated to production of X-radiation. Measurements were made on beam lines 7-3 and 6-2. At CHESS we used the A-2 line while X-rays were produced under colliding beam ( $e^-, e^+$ ) conditions with typical currents of 50–100 mA at 5.2 GeV. All rhenium measurements (10.219–11.283 KeV,  $L_{III}$  edge at 10.5306 KeV) reported were made at SSRL, whereas those for tin (28.895–30.721 KeV, K edge at 29.195 KeV) were carried out at CHESS.

Fluorescence and transmission spectra were usually measured simultaneously. Ionization chambers were used as the X-ray detector for  $I_0$  (incident),  $I_t$  (transmission), and  $I_c$  (calibrant transmission). The ionization chamber of the fluorescence detector<sup>16</sup> was always filled with argon gas. Rejection of scattered X-ray photons was achieved with foil filters. For Re EXAFS, a Cu (20  $\mu\text{m}$ ) foil was used to absorb scattered photons and a Cd (125  $\mu\text{m}$ ) foil was used for Sn-EXAFS. The fluorescence detector was fitted with a Soller slit system to reject fluorescence photons from the filter foil. A rhenium metal flake sample was used as the energy calibrant for Re EXAFS, and a tin metal foil (25  $\mu\text{m}$ ) was used for Sn EXAFS. All spectra were measured in scanning mode. To improve the statistics of the data, 10 to 20 scans were collected on each sample and subsequently averaged.

Data collection utilized the local software at each site. A typical spectrum started at 300 eV before the edge and went as high as  $19.0 \text{ \AA}^{-1}$ . To obtain high quality EXAFS at high regions in  $k$ -space, samples were cooled to 10 K during data collection if possible. At SSRL, low temperature was obtained using a flowing liquid helium cryostat (Oxford

(10) Martin, J. L.; Yuan, J.; Deutsch, K.; Elder, R. C.; Heineman, W. R.; Deutsch, E. *J. Nucl. Med.* **1990**, *30*, 732a.

(11) Pipes, D. W.; D'Amore, J.; Deutsch, K.; Elder, R. C.; Deutsch, E. *J. Nucl. Med.* **1991**, *32*, 1089a.

(12) Pipes, D. W.; Yuan, J.; Helmer, B.; Deutsch, K.; Elder, R. C.; Deutsch, E. *J. Nucl. Med.* **1993**, *34*, 120p.

(13) Ram, M. S.; Hupp, J. T. *Inorg. Chem.* **1991**, *30*, 130.

(14) Chen, B.; Heeg, M. J.; Deutsch, E. *Inorg. Chem.* **1992**, *31*, 4683.

(15) Vejgele, W. J. *At. Data* **1973**, *5*, 51.

(16) EXAFS Co., Seattle WA Stern, E. A.; Heald, S. M. *Rev. Sci. Instrum.* **1979**, *20*, 627.

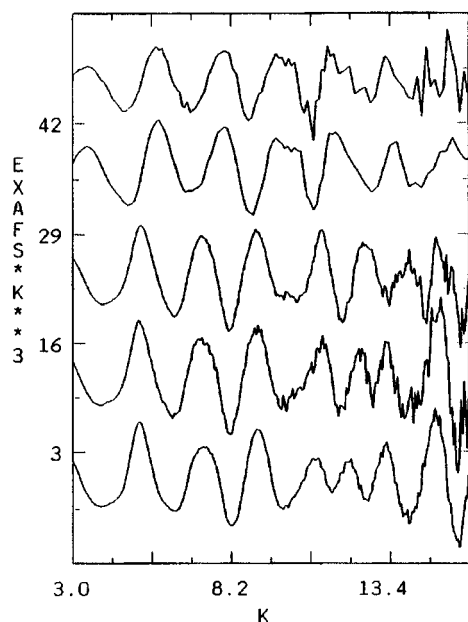


**Figure 1.** Re  $L_{III}$  EXAFS data (raw  $\chi(k)$ ,  $k^3$  weighted): lowest trace, (H-Sn) ReHEDP; second lowest trace, (Clin) ReHEDP; middle trace, (L-Sn) ReHEDP. Sn K EXAFS data (raw  $\chi(k)$ ,  $k^3$  weighted): second from top trace, (L-Sn) ReHEDP; top trace, Sn(IV)ReHEDP.

Instruments). At CHESS, a closed-cycle, helium refrigerator (Displex, Air Products Inc.) was used.

**EXAFS Extraction and Fourier Transformation.** EXAFS data analyses and least-square refinements were performed by standard methods<sup>17</sup> using XFPK<sup>18</sup> with local modifications. The preedge was fit to a straight line in the range  $-200$  eV to  $-50$  eV, and the extrapolated values were subtracted from the data. EXAFS data,  $k$ , were extracted using four, equal length, cubic spline segments. Normalization was based on the spline value at  $k = 0.0 \text{ \AA}^{-1}$ . Raw data files (10–20 scans for each sample) were averaged. The endpoints for Fourier transformations (FT) were chosen to coincide with the EXAFS nodes to minimize the cut-off effect. The raw Re  $L_{III}$  EXAFS data from three different aqueous solutions of (H-Sn) ReHEDP, (L-Sn) ReHEDP, and (Clin) ReHEDP and also the Sn K EXAFS data for two solid samples of (H-Sn) ReHEDP and Sn(IV)HEDP are shown in Figure 1 together with their  $k^3$  weighted Fourier transforms (FT) using EXAFS data in range  $3.3\text{--}16.4 \text{ \AA}^{-1}$  in Figure 2. For the FT of Sn K EXAFS a limited  $k$ -range of  $3\text{--}14.5 \text{ \AA}^{-1}$  was used due to the high noise level in the raw data at the higher values of  $k$ .

To test whether the FT peaks at  $2.0 \text{ \AA}$  and above in Figure 1 resulted from heavy back scatterers, the FTs were recomputed using different ranges in  $k$  of the EXAFS data. Figure 3 shows three different transforms for (H-Sn) ReHEDP computed using different ranges in  $k$  space:  $3.3\text{--}16.4 \text{ \AA}^{-1}$  (bottom);  $7.8\text{--}16.4 \text{ \AA}^{-1}$  (middle); and  $3.3\text{--}13.0 \text{ \AA}^{-1}$  (top).

**Reference Compounds.** Based on chemical information available concerning the complexes of interest and preliminary EXAFS analyses, the EXAFS data from various reference complexes of known crystal structure were used to extract phase and amplitude functions for particular back scatterers. For Re—O,  $\text{NH}_4\text{ReO}_4$  with four oxygen atoms at  $1.74 \text{ \AA}$  was used.<sup>19</sup> For Re—Re, rhenium metal was used with 12 neighbors at an average of  $2.76 \text{ \AA}$ .<sup>20</sup>

Each particular back scatterer was isolated by computing the  $k^3$  weighted FT in the approximate  $k$  range from  $3$  to  $16 \text{ \AA}^{-1}$  and then taking the inverse FT of the peak of interest. The actual  $k$  range was chosen to match that of the data to be fitted. The endpoints for the

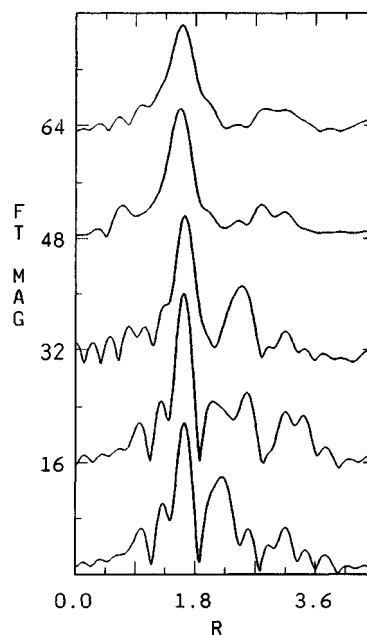


**Figure 2.** Fourier transforms (magnitude plotted vs phase-shifted distance,  $k^3$  weighting). The trace order of samples is the same as in Figure 1. Re data,  $\Delta k = 3.3\text{--}16.5 \text{ \AA}^{-1}$ ; Sn data,  $\Delta k = 3.3\text{--}14.5 \text{ \AA}^{-1}$ .

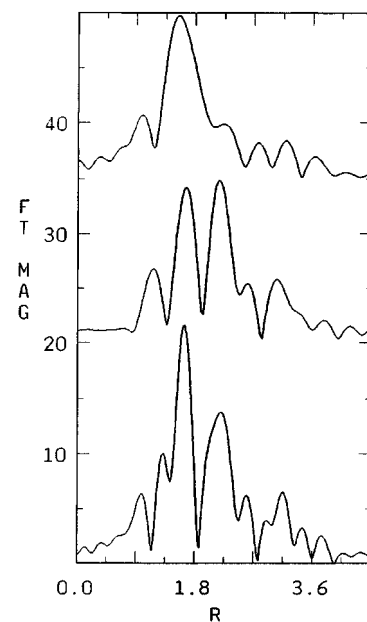


**Figure 3.** Fourier transforms Re  $L_{III}$  EXAFS of (H-Sn) ReHEDP weighted by  $k^3$ : bottom trace,  $\Delta k = 3.3\text{--}16.3 \text{ \AA}^{-1}$ ; middle trace,  $\Delta k = 7.7\text{--}16.3 \text{ \AA}^{-1}$ ; top trace,  $\Delta k = 3.3\text{--}13.0 \text{ \AA}^{-1}$ .

inverse FT were chosen at the points where the imaginary part of the FT has nodes.<sup>21</sup>

For Re—Sn, no well characterized reference material was available and so all calculations for this back scatterer utilized theoretical phases and amplitudes generated by the FEFF5 program.<sup>22</sup> The Sn(IV)HEDP complex was prepared to provide a comparison standard based on its Sn EXAFS relative to the Sn EXAFS obtained from tin present in the various ReHEDP preparations.

**Filtering and Curve Fitting.** Isolated peaks from the FTs were back transformed as described above to yield filtered EXAFS. In general where intercomparison between two similar materials was desired, the back transform conditions were kept the same. All curve

(17) Sayers, D. E.; Bunker, B. E. In *X-Ray Absorption*; Koningsberger, D. C., Prins, R., Eds.; Wiley: New York, 1988; p 211. Watkins, J. W.; Elder, R. C.; Greene, B.; Darnall, D. W. *Inorg. Chem.* **1987**, *26*, 1147.  
 (18) Scott, R. A. *Methods Enzymol.* **1985**, *117*, 414.  
 (19) Brown, R. J. C.; Segal, S. L.; Dolling, G. *Acta Crystallogr.* **1980**, *B36*, 2195.  
 (20) Wyckoff, R. W. G. *Crystal Structures*; Wiley: New York, 1963; Vol. 1, p 11.

(21) van Zon, J. B. A. D.; Koningsberger, D. C.; van't Blik, H. F. J.; Sayers, D. E. *J. Chem. Phys.* **1985**, *82*, 5742.  
 (22) Rehr, J. J.; Albers, R. C.; Zabinsky, S. I. *Phys. Rev. Lett.* **1992**, *69*, 3397.

fitting was based on least squares minimization using  $k^3$  weighted data. The number of parameters used in a one shell fit is four ( $R$ , interatomic distance;  $N$ , coordination number;  $\sigma$ , disorder parameter and  $\Delta E_o$  shift in energy of  $k = 0$ ). The statistically justified number of fitting parameters is estimated from the Nyquist theorem,  $n = 2\Delta k\Delta R/\pi$ , where  $\Delta k$  and  $\Delta R$ , respectively, are the  $k$  and  $R$  ranges used in the forward and inverse Fourier transformations.<sup>23</sup> In general, multishell fits were constrained so as not to exceed this number of variables. Errors were calculated as the difference between the best fit value of a given variable for all variables refined and that value which doubles the residual when all variables except the one in question are refined.<sup>23</sup>

**Processing of Overlapping Peaks.** The lower two Fourier transforms in Figure 2 demonstrate the result of two peaks overlapping<sup>17</sup> producing a sharp minimum at  $r = 1.9 \text{ \AA}$ . Generally, large errors are expected if an attempt is made to separately back transform the interfering peaks. This difficulty can be alleviated somewhat if the overlapping peaks are from back scatterers of quite different atomic numbers. Low  $Z$  atoms as back scatterers tend to cause the EXAFS to peak at low values in  $k$  space, whereas high  $Z$  atoms peak at higher  $k$  space values. Since in this case the first shell back scatterer was from oxygen neighbors and the second shell appeared to result from back scatterer from heavy atom neighbors, the FT was recomputed using the range in  $k$  space of  $3.3\text{--}13.0 \text{ \AA}^{-1}$ , emphasizing the low  $R$  peak and reducing the high  $R$  peak. The low  $R$  peak was then filtered using the range  $1.0\text{--}2.0 \text{ \AA}$  with a Gaussian window of  $0.3 \text{ \AA}$ . The Re–O model parameters were derived using this range of data as well.

For each of the materials examined, any peak above  $2.0 \text{ \AA}$  was examined by computing FTs from two different data ranges,  $3.3\text{--}16.4 \text{ \AA}^{-1}$  and  $7.8\text{--}16.4 \text{ \AA}^{-1}$ . The full range of EXAFS data was used for computing the transform which was subsequently filtered and fit as a second shell.

## Results and Discussion

**Rhenium–Oxygen Interactions.** One and two shell optimizations of the EXAFS were used to investigate four materials: (Subs) ReHEDP, (L–Sn) ReHEDP, (H–Sn) ReHEDP, and (Clin) ReHEDP. (Subs) ReHEDP appears quite different from the other three materials as might be expected from its qualitatively different preparation. Its precursor, *trans*-[py<sub>4</sub>(O)<sub>2</sub>-Re]<sup>+</sup>, has Re in the +5 oxidation state and is rather unlikely to have been oxidized or reduced in the substitution process.

The FT for (Subs) ReHEDP is shown in Figure 4. The principal peak at  $1.6 \text{ \AA}$  in the pseudoradial distribution function (PRDF) clearly results from back scatter by a first shell of oxygen atoms. A single shell fit of the filtered data gives  $5 \pm 3$  oxygen atoms at a distance of  $2.0 \pm 0.1 \text{ \AA}$ , with the disorder parameter  $\sigma = 0.06 \text{ \AA}$  and  $\Delta E_o = 18.4 \text{ eV}$ . However, the fit is rather poor with a goodness of fit ( $F$ ) of 0.47.

$$F = \left\{ \sum [k^3(\chi_{\text{obs}} - \chi_{\text{calc}})]^2 / N_{\text{pts}} \right\}^{1/2} \text{ over all data points}$$

A two-shell fit allowing for a short yl oxygen distance as well as the longer single bonded value refines to  $1.4 \pm 0.7$  oxygens at  $1.76 \pm 0.04 \text{ \AA}$  with  $\sigma = 0.05 \text{ \AA}$  and  $\Delta E_o = -6.0 \text{ eV}$  for the yl oxygens and  $4.5 \pm 1.5$  single-bonded oxygens at  $2.07 \pm 0.02 \text{ \AA}$  with  $\sigma = 0.07 \text{ \AA}$  and  $\Delta E_o = 5.3 \text{ eV}$  with the remarkably better fit of 0.05. Thus it seems clear that at least one and possibly both of the yl oxygen atoms of the starting material remain in the (Subs) ReHEDP product.

For the other three materials, all produced by stannous reduction of perrhenate in the presence of excess ligand, no evidence could be found by fitting of any significant amount of yl oxygen ( $n < 0.2$ ). It may well be that these contain rhenium in an oxidation state less than +5. This conclusion is further supported by the presence of a short Re–Re distance (vide infra).

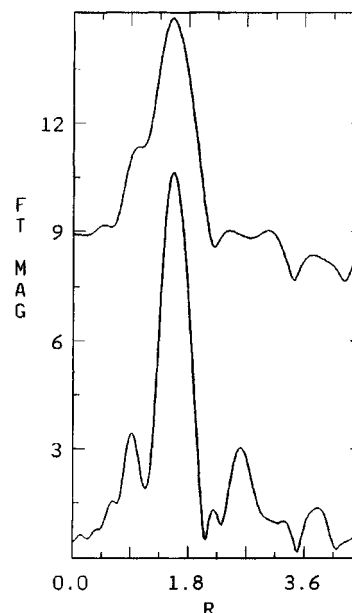


**Figure 4.** Fourier transforms of (Subs) ReHEDP calculated using  $\Delta k = 3.0\text{--}16.4 \text{ \AA}^{-1}$  (lower trace) and  $\Delta k = 7.2\text{--}15.6 \text{ \AA}^{-1}$  (upper trace). The prominent peak at *ca.*  $1.5 \text{ \AA}$  can best be fit by both an yl oxygen distance and also a longer single bonded Re–O distance. The disappearance of the peak at *ca.*  $2.5 \text{ \AA}$  in the upper trace indicates there is no heavy back scatterer as a near neighbor to Re in this material.

**Table 1.** Structural Parameters of the Oxygen Coordination Shells in ReHEDP Samples, Determined by Single- and Two-Shell Fit

	H-Sn		Clin		L-Sn
	Single-Shell Fit				
$R, \text{ \AA}$	2.03(1) <sup>a</sup>		2.04(1)		2.04(1)
$N$	6.6(9)		6.6(9)		5.5(7)
$\sigma, \text{ \AA}$	0.06		0.05		0.035
$\Delta E_o, \text{ eV}$	3.2		3.5		0.7
$F$	0.34		0.22		0.15
	Two-Shell Fit <sup>b</sup>				
$R, \text{ \AA}$	1.979(5)	2.092(5)	1.975(2)	2.065(2)	did
$N$	3.1(2)	3.1(2)	1.9(5)	4.6(6)	not
$\sigma, \text{ \AA}$	0.000	0.000	0.000	0.028	improve
$F$	0.24		0.19		

<sup>a</sup> Errors, where they have been calculated, are given in parentheses and represent the uncertainty in the least significant digit. <sup>b</sup> For the two-shell fit, the values of  $\Delta E_o$  were fixed at the values found in the single shell treatment to keep the maximum number of refined variables at six.

For the three samples produced by reduction with stannous ion, structural results are summarized in Table 1. First a single shell was fit for Re–O. These gave reasonable results with approximately six oxygen atoms at a distance of  $2.04 \text{ \AA}$ . However the fits could be significantly improved for the high tin and clinical samples using a two shell fit.<sup>24</sup> The total coordination number remained approximately six. The distances for the high tin and the clinical samples indicate two different distances one of  $1.97 \text{ \AA}$  and another at  $2.08 \text{ \AA}$ . For the low tin sample a two-shell model did not refine to significantly different distances nor give rise to a significantly better fit.

**Raman Spectra.** For (Subs) ReHEDP the presence of an yl oxygen atom was confirmed by the Raman spectrum. The Re=O stretch at  $1022 \text{ cm}^{-1}$  is the strongest band in that spectrum with other bands at  $1609$  (61%),  $1069$  (23%),  $899$  (8%),  $792$  (10%),  $718$  (9%),  $648 \text{ cm}^{-1}$  (35%) where the number in parentheses is the band intensity relative to the  $1022 \text{ cm}^{-1}$  band.

(23) Lytle, F. W.; Sayers, D. E.; Stern, E. A. *Physica B* **1989**, *58*, 701.

(24) Joyner, R. W.; Martin, K. J.; Meehan, P. J. *Phys. C: Solid State Phys.* **1987**, *20*, 4005.

**Table 2.** Re–Re Interactions Based on  $k = 3.3\text{--}16.4 \text{ \AA}^{-1}$ 

parameters	H-Sn	L-Sn	Clin	
$R, \text{ \AA}$	2.40(3)	2.75(6)	2.35	2.80
$N$	1.3(7)	2.2(9)	0.8	1.3
$\sigma, \text{ \AA}$	0.036	0.045	0.034	0.038
$\Delta E_0, \text{ eV}$	9.4	27.2	11.5	9.3
$F$	0.26	0.20	0.33	
$\Delta R,^a \text{ \AA}$	1.9–2.5	2.2–2.8	1.9–2.8	

<sup>a</sup>  $\Delta R$  is the range of the back transformation to yield the filtered EXAFS for each material.

For comparison the bands for the *trans*-dioxo Re(V) complex, [(py)<sub>4</sub>(O)<sub>2</sub>Re]Cl, are found at 1609 (43%), 1223 (9%), 1072 (11%), 1018 (100%) 912 (3%), 648 cm<sup>-1</sup> (29%), and those for the monooxo Re(V) complex, [Ph<sub>4</sub>As][ReO(DBDS)], are recorded at 1574 (65%), 1401 (20%), 1320 (16%), 1184 (26%), 1080 (17%), 1018 (26%), 999 (100%), 968 (41%), 721 (15%), 667 (30%), 490 (18%), and 455 cm<sup>-1</sup> (21%). Unfortunately we were unable to obtain acceptable spectra for the three tin-reduced specimens of ReHEDP.

**Rhenium–Rhenium Interactions.** As can be seen from Figure 2 and Figure 4 the PRDFs for all four ReHEDP materials show significant peaks beyond those from the coordinated oxygen atoms.

The (Subs) ReHEDP material is rather different from the three other samples. Figure 4 shows the FTs computed both using the entire range of data (3.0–15.6  $\text{ \AA}^{-1}$ , lower trace) and using only the high  $k$  data (7.2–15.6  $\text{ \AA}^{-1}$ , upper trace). The peak at *ca.* 2.5  $\text{ \AA}$  in the PRDF with full data vanishes in the recomputed function, indicating that it results from a combination of low  $Z$  atoms and/or noise. Back transformation of this peak shows filtered EXAFS characteristic of low  $Z$  back scatterers as well. Thus, there is no evidence in the (Subs) ReHEDP material for the presence of any Re–Re interactions.

The three materials produced by tin reduction of perrhenate all show evidence of Re–Re interactions. Both the high Sn and low Sn samples show what appear to be single peaks in the range 1.9–2.5  $\text{ \AA}$  for the former and 2.2–2.8  $\text{ \AA}$  for the latter. The clinical sample shows two peaks in the range 1.9–2.8  $\text{ \AA}$ . Back transformation of these peaks indicates that they result from back scatter by rhenium neighbors (see below for evidence that these are not tin neighbors). The results of fitting the filtered EXAFS are given in Table 2.

In the high tin and the low tin samples, the Re–Re distances are quite different. On the basis of the large number of metal–metal bonded species known for rhenium<sup>25</sup> and also the amounts of reducing agent present in each case, it seems likely that both materials are reduced below the +5 oxidation state of the (Subs) ReHEDP material, and that the high tin sample is in the lowest oxidation state with the low tin material in a somewhat higher oxidation state.

The clinical sample shows clear indications of both types of Re–Re bond and was fit by two shells. The two refined distances are in quite good agreement with the individual distances from the high tin and low tin samples.

In an effort to determine whether the high and low tin samples might contain some admixture of both the short and long Re–Re bonds, the data were transformed over the  $k$  range of 7.8–16.4  $\text{ \AA}^{-1}$  (to emphasize the Re back scatter versus any from low  $Z$  atoms), and the range from 1.9 to 2.8  $\text{ \AA}$  was reverse transformed to include any contributions from either type of bond. The resulting two shell fits are given in Table 3.

**Table 3.** Re–Re Interactions Based on  $k = 7.8\text{--}16.4 \text{ \AA}^{-1}$ 

parameters	H-Sn		L-Sn		Clin	
$R, \text{ \AA}$	2.40 <sup>a</sup>	2.81	2.32	2.79	2.39	2.81
$N$	1.2	0.5	0.3	1.5	0.8	1.5
$\sigma, \text{ \AA}$	0.03	0.04	0.03	0.04	0.03	0.04
$\Delta E_0, \text{ eV}$	7.9	5.1	8.8	8.6	9.7	7.1
$F$	0.39		0.38		0.40	

<sup>a</sup> The same range ( $\Delta R = 1.9\text{--}2.8 \text{ \AA}$ ) was used for all samples in calculating the inverse FT; the range of data available justified a maximum of four fitting parameters. Parameters were varied in blocks (1st  $\Delta E_0$  and  $N$  from each shell, 2nd  $N$  and  $R$  from each shell, 3rd  $R$  and  $\sigma$  from each shell, 4th repeat 2nd step) with all other parameters held fixed. Thus, no more than four parameters were varied simultaneously.

That the distances remained in fair agreement with the previously found values, suggests that there is some admixture. Values of  $n$ , the number of neighbors, indicate for the high tin sample that the short bond predominates by 2:1 whereas for the low tin the long bond is favored 4:1. The clinical sample also favors the long bond, but only by 2:1. Also it is worth noting that the number of metal–metal bonds per rhenium atom is quite similar for all three tin-reduced samples.

**Rhenium–Tin Interactions.** The measurements of SnHEDP and ReHEDP made near the tin K edge (29.195 keV) were used to search for a rhenium–tin interaction. The use of stannous ion reducing agent with technetium or rhenium plus added HEDP ligand has led to a tight association with tin in the final radiopharmaceutical complex. One possibility is that in the electron transfer process a complex is formed in which the product Sn(IV) is bound to the Re center by means of an oxygen bridge. A specific example of this type of bridging to technetium in a tris(dimethylglyoxime) complex was shown many years ago,<sup>26</sup> and a modified form has been reported more recently.<sup>27</sup>

Such a bridge system could result in a Re–Sn distance as short as 2.7  $\text{ \AA}$  and might be observable in the EXAFS spectrum. In fact the FTs of Sn(IV)HEDP and Sn in (L-Sn) ReHEDP shown in Figure 2 (top two traces) look remarkably similar. Although measurements were made at 10 K, no strong evidence of peaks close beyond a first shell of oxygen atoms around tin is recorded in either FT (compare to lower three traces in Figure 2). Depending on the bridge angle the Re–Sn distance could be between 2.7 and 4.0  $\text{ \AA}$  and might not be observable via EXAFS. The peaks in Figure 2 at 2.7 and 3.2  $\text{ \AA}$  may result at least in part from heavy back scattering. However, they occur where there is a minimum in the FTs computed from Re EXAFS.

This comparison is made explicit in Figure 5. Here the Fourier transforms of Re EXAFS and Sn EXAFS from the same (L-Sn) ReHEDP sample are plotted. The Re PRDF (lower trace) shows a significant second peak near 2.4  $\text{ \AA}$  which we were able to fit equally well as arising from Re–Re or from Re–Sn. The Sn PRDF (upper trace) shows no peak in the same region (neither a strong Sn–Sn nor Sn–Re), and thus we believe the peak in Re PRDF must come from a Re–Re interaction and that no significant Re–Sn interactions occur in these materials.

**Structure Insights.** The multiple EXAFS measurements and fits as well as the analytical and Raman data may be interpreted in terms of the following structural formulations for the various materials studied.

(25) Cotton, F. A.; Walton, R. *Multiple Bonds Between Metal Atoms*, 2nd ed.; Oxford Press: Oxford, UK, 1993; pp 28–138.

(26) Deutsch, E.; Elder, R. C.; Lange, B. A.; Vaal, M. I.; Lay, D. G. *Proc. Natl. Acad. Sci. U.S.A.* **1976**, *73*, 4287.

(27) Linder, K. E.; Malley, M. E.; Gougoutas, J. Z.; Unger, S. E.; Nunn, A. D. *Inorg. Chem.* **1990**, *29*, 2428.

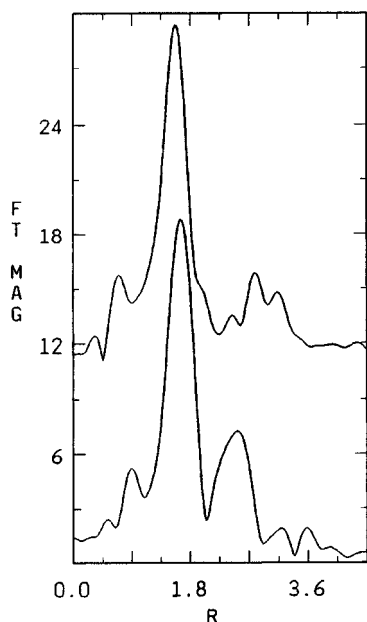


**Figure 5.** Fourier transforms of Re L<sub>III</sub> and Sn K EXAFS of the same sample, (L-Sn) ReHEDP. The lower trace (Re EXAFS) shows a heavy neighbor at ca. 2.4 Å, while the upper trace (Sn EXAFS) shows no equivalent peak. Thus there can only be a Re–Re interaction

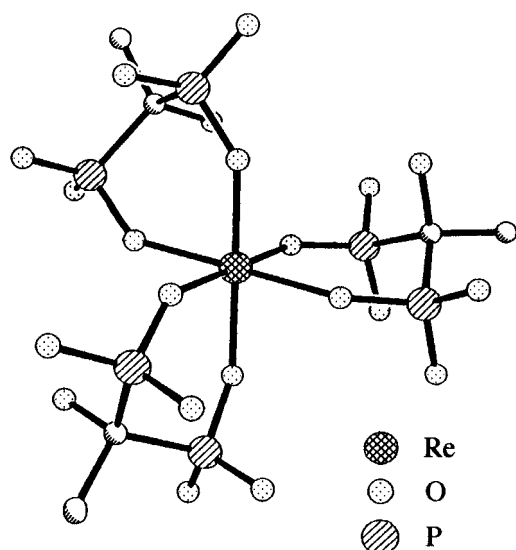


**Figure 6.** A possible structure for the anion,  $[\text{Re}(\text{H}_2\text{HEDP})_3]^-$ , in the (Subs) ReHEDP material.

**(Subs) ReHEDP.** The analytical data show the presence of considerable nitrogen (presumably from intact pyridine ligands). The atomic ratios for this material are as follows: Re, 1.0; C, 20.4; H, 35.6; N, 3.2; P, 4.6; Cl, <0.03. Since the synthesis was conducted in anhydrous ethanol under an inert atmosphere, it seems reasonable that the rhenium remains in the +5 oxidation state. Also since  $\text{H}_4\text{HEDP}$  was used it seems likely that the  $[\text{H}_2\text{HEDP}]^{2-}$  dianion is the form of the ligand to bind to rhenium. Three ligands would then form the  $[\text{Re}(\text{H}_2\text{HEDP})_3]^-$  monoanionic complex. A structure of this type is shown in Figure 6. In anhydrous ethanol and in the presence of  $\text{trans}-(\text{py})_4(\text{O})_2\text{Re}^+$ , the 1:1 salt,  $[(\text{py})_4(\text{O})_2\text{Re}][\text{Re}(\text{H}_2\text{HEDP})_3]$ , is likely to precipitate.

This hypothesis, which with 1 mol each of ethanol and pyridine as solvent of crystallization per rhenium atom, would give the following atom ratios: Re, 1; C, 20; H, 30; N, 3; P, 3 in moderate agreement with the analytical figures. The Raman data show a spectrum which is very similar to but slightly shifted

from that of the  $\text{trans}-(\text{py})_4(\text{O})_2\text{Re}^+$  starting material suggesting that the cation is intact but in a slightly different matrix.

The EXAFS data for such a substance superimpose both the anion and the cation, *i.e.*, they show the average rhenium environment. The fit of the first neighbor peak was to two shells of  $1.4 \pm 0.7$  oxygen atoms at  $1.76 \pm 0.04$  Å and  $4.5 \pm 1.5$  oxygens at  $2.07 \pm 0.02$  Å. Clearly the first shell agrees with the *trans*-dioxo fragment of  $\text{trans}-(\text{py})_4(\text{O})_2\text{Re}^+$ . The second shell is in good agreement with the composite of 4 nitrogen atoms at an average of 2.14 Å and six terminal oxygen atoms from the  $[\text{Re}(\text{H}_2\text{HEDP})_3]^-$  anion at ca. 1.98 Å. The increased value of the disorder parameter,  $\sigma = 0.07$  Å, provides further agreement that the second shell is really the superposition of two further sub shells where nitrogen and oxygen can both be satisfactorily fit using oxygen back scattering functions.

As shown in Figure 4, there are no Re–Re interactions in (Subs) ReHEDP which again agrees with the hypothesis that this material may be formulated as composed of isolated  $\text{trans}-(\text{py})_4(\text{O})_2\text{Re}^+$  cations and  $[\text{Re}(\text{H}_2\text{HEDP})_3]^-$  anions. It is possible that the pyridine freed in the reaction would be protonated and could serve as the counterion in the precipitation of the tris( $\text{H}_2\text{HEDP}$ ) rhenium anion. However this would lower the amount of yl oxygen found in the precipitate and is in disagreement with the EXAFS data. Although more crystal structures seem to have been reported for tris bidentate chelate complexes of rhenium(VI) (tris(3,5-di-*tert*-butylcatecholato)rhenium(VI),<sup>28</sup> tris(tetrachlorocatecholato)rhenium(VI) anisole solvate,<sup>28</sup> and tris(*o*-phenylenediamide-*N,N'*)rhenium(VI) tetrahydrofuran solvate<sup>29</sup>), a rhenium(V) example is also known (pseudo-benzoquinonediimide-*N,N'*)bis(*o*-phenylenediamide-*N,N'*)rhenium(V) tetrahydrofuran solvate<sup>29</sup>).

**Tin-Reduced Complexes of ReHEDP.** The experimental results show major differences between these materials and (Subs) ReHEDP. They differ as follows: (1) relatively short Re–Re interactions are found in the EXAFS of the reduced materials but not in (Subs) ReHEDP; (2) Re=O bonds seen in (Subs) ReHEDP are absent from the tin reduced materials; (3) the reduced materials contain tin:rhenium in approximately a 1:1 ratio, and tin is not separated from the Re complex by chromatographic purification, whereas no tin is present in (Subs) ReHEDP; (4) there are approximately 3 HEDP ligands per 1 Re in the tin-reduced materials and only half that amount in (Subs) ReHEDP; (5) lithium ions are present in the tin-reduced materials at approximate ratios of 5:1Li:Re and are missing from (Subs) ReHEDP; and (6) the tin-reduced materials were synthesized in aqueous media whereas (Subs) ReHEDP was synthesized in absolute ethanol.

Based on these observations, five generalizations may be made about all of the tin-reduced materials. First, the complexes are oligomeric with Re–Re bonds. This is based primarily on the EXAFS results showing relatively short Re–Re distances (range = 2.4–2.8 Å).

Second, the rhenium is likely in a lower oxidation state than +5. Several observations bear on this. The lack of Re=O bonds in the EXAFS, the excess of tin reducing agent, and the short Re–Re distances all combine to suggest reduction below the Re(V) state expected for (Subs) ReHEDP.

Third, the diphosphonate ligands form bridges between rhenium and tin. That the preparative DEAE chromatography does not separate tin and rhenium species suggests some covalent linkage. However, the possibility of an oxo or hydroxo

(28) deLeairie, L. A.; Haltiwanger, R. C.; Pierpont, C. G. *Inorg. Chem.* **1987**, *26*, 817.

(29) Danopoulos, A. A.; Wong, A. C. C.; Wilkinson, G.; Hursthouse, M. B.; Hussain, B. *J. Chem. Soc., Dalton Trans.* **1990**, 315.

bridge between rhenium and tin is eliminated by the tin EXAFS results which show no metal neighbors for tin at less than 4.0 Å.

Fourth, it is unlikely that the first coordination sphere contains ligating atoms other than diphosphonate or hydroxyl oxygen atoms. The EXAFS results show that all of the first neighbor atoms are light, i.e., nitrogen or oxygen. No nitrogen donors were present in the reaction or workup mixtures, and thus the bound atoms are oxygen. The bond lengths found admit neither the possibility of an oxo group (which would be a shorter bond length than found) or bound water (which would have a longer bond length than found).

Fifth, although the HEDP ligand is most likely to be fully ionized to yield the tetraanionic species for syntheses conducted in aqueous media,<sup>30</sup> and the tin is certainly in the +4 state, the analytical results for both the number of ligands and lithium cations are too uncertain to use charge counting to assess the rhenium oxidation state. The individual cases are discussed below.

**ReHEDP (H-Sn).** Here the Re—Re distance is 2.40 Å, the shortest observed for any of the tin-reduced materials, which suggests the lowest oxidation state for rhenium in any of these systems. This also agrees with the use of a large excess of the tin reducing agent in preparing this material. The Re—Re coordination number of  $1.3 \pm 0.7$  is rather uncertain but indicates the degree of polymerization. For a dimer this number is 1.0, for an infinite chain length species or a cyclic species the number is 2.0, and for a tetrahedral cluster of rhenium atoms it is 3.0. In the case of a linear trimer, the two terminal rhenium atoms have one Re neighbor, and the central Re has two Re neighbors, giving an average Re—Re coordination number of 1.33.

Additional information about the polymerization number is obtained from the number of Re—O groups found with one of two different distances, one set for bridging and the other for terminal Re—O. In the case of ReHEDP (H-Sn), consider the linear polymeric structure (assuming that there are two bridging oxygens, which seems to be generally the case with this type of ligand); a terminal Re will have 4 Re—O<sub>term</sub> and 2 Re—O<sub>br</sub>, while the interior Re will have 2 Re—O<sub>term</sub> and 4 Re—O<sub>br</sub>. There will always be 2 terminal rhenium atoms in this type of structure, and there will be  $n - 2$  interior atoms. Thus there are  $[2 \times 4 + (n - 2) \times 2]$  Re—O<sub>term</sub> and  $[2 \times 2 + (n - 2) \times 4]$  Re—O<sub>br</sub>. To get the average number of each bond type per rhenium, divide by  $n$ . The results are dimer: term = 4.0, br = 2.0; trimer: term = 3.33, br = 2.67; tetramer: term = 3.0, br = 3.0; pentamer: term = 2.8, br = 3.2. The result for ReHEDP (H-Sn) of Re—O<sub>br</sub> =  $3.1 \pm 0.2$  and Re—O<sub>term</sub> =  $3.1 \pm 0.2$  suggests a tetramer to be the most likely structure. Given the uncertainty in the calculation of a trimer based on the Re—Re coordination number (Re—Re =  $1.3 \pm 0.7$ ), we have chosen to model a tetrameric structure.

A possible tetrameric framework structure is shown in Figure 7a. The framework structure is based on octahedral coordination about Re with four rhenium atoms bridged into a linear structure by edge sharing of the octahedra. The Re—Re distances are adjusted to 2.4 Å with Re—O<sub>term</sub> = 1.97 Å and Re—O<sub>br</sub> = 2.03 Å. Figure 7b illustrates attachment of two HEDP ligands in *trans* opposition in the horizontal plane and two others in opposition in the vertical plane, all to the front of the view of the tetramer. Figure 7c shows the manner in which a tin atom already bound by a tetradentate HEDP ligand can then bind to

two oxygen donors from a second HEDP which is bound to rhenium. Note that in all cases where the HEDP is coordinated through four oxygen atoms, the remaining two noncoordinated oxygen atoms are those in the planar fragment O—P—C—P—O. This appears typical when four of the oxygen atoms of the HEDP ligand are coordinated.<sup>31</sup>

Figure 7d illustrates the progression from 7b by the further binding of four more HEDP ligands to the rhenium skeleton and the additional binding of four SnHEDP moieties as in 7c to complete the structure. Lithium ions (presumably hydrated) would be expected to interact with the remaining negative sites on the diphosphonate ligands.

The choices made, while in agreement with all the observations, still are somewhat arbitrary in that no HEDP ligand is bound solely to one rhenium atom whereas each tin atom has four of its coordination sites filled by a single HEDP which does not bind to any other metal atom. Also the conformational choices for the arrangement of the HEDP ligands are arbitrary with respect to bending up or down from the horizontal plane except that a relatively symmetric disposition has been chosen.

Finally, the linear tetramer model requires five oxygen atom donors on each side of the line of rhenium atoms (see Figure 7a), two terminal and three bridging. The two HEDP ligands in the horizontal plane on each side of the line of rhenium atoms supply four of these. The remaining oxygen atom on each side is most easily supplied as a hydroxyl moiety. If it is placed in the center of the line of five oxygen donors as a hydroxo bridge, then the structure is more symmetrical, the crowding in the center of the structure is reduced, and each end is composed of a separate dimer unit. For the tetramer to dissociate to two dimers, all that is required is to break one of the bridging bonds for each hydroxyl and to add water to fill in the vacant coordination position.

The point of this model is not to hypothesize *the* structure for (H-Sn) ReHEDP, but rather to show that all of the available evidence is in agreement with a straightforward structural model. In fact, it appears unlikely that these materials correspond to a single formulation. More likely, they are complex mixtures of low oligomer numbers in the range of 2–5.

**(L-Sn) ReHEDP.** Here the Re—Re coordination number is  $2.2 \pm 0.9$  and the Re—Re distance is longer  $2.75 \pm 0.06$  Å, suggesting a higher rhenium oxidation state on average than ReHEDP (H-Sn). However, this distance is still within the bonded Re—Re range. The Re—Re coordination number of 2.2 suggests a cyclic structure (*vide supra*). For a trinuclear cluster the Re—Re coordination number is 2.0.

Thus we have chosen a triangular cluster model for (L-Sn) ReHEDP. This model has two Re—O bridges and four Re—O terminal groups. However, this postulate concerning the bridging to terminal ratio proved untestable as there was no improvement for a two-shell fit over a single shell fit of the Re—O distances for ReHEDP (L-Sn). In this model, shown in Figure 8, the most distinctive feature is the presence of two capping ligands above and below the triangular cluster of rhenium atoms. Each cap uses a PO<sub>3</sub> group from HEDP and binds each oxygen atom in turn to one of the three rhenium atoms. Similar capped triangular structures have been observed for Re<sub>3</sub> clusters with PO<sub>4</sub><sup>3-</sup>, AsO<sub>4</sub><sup>3-</sup>, and SO<sub>4</sub><sup>2-</sup> ligands.<sup>32</sup>

(30) Krol, I. A.; Tolkacheva, E. O.; Starikova, Z. A.; Popov, K. I. *Koord. Khim.* **1990**, *16*, 1621. Krol, I. A.; Starikova, Z. A.; Tolkacheva, E. O. *Zh. Strukt. Khim.* **1991**, *32*, 159.

(31) Krol, I. A.; Starikova, Z. A.; Sergienko, V. S.; Tolkacheva, E. O. *Zh. Neorg. Khim.* **1990**, *35*, 2817. Krol, I. A.; Starikova, Z. A.; Tolkacheva, E. O.; Sergienko, V. S.; Makarevich, S. S. *Zh. Neorg. Khim.*, **1992**, *37*, 304. Sergienko, V. S.; Tolkacheva, E. O.; Ilyukhin, A. B.; Starikova, Z. A. Krol, I. A. *Mendeleev Commun.* **1992**, 144.  
(32) Irmeler, M.; Meyer, G. Z. *Anorg. Allg. Chem.* **1990**, *587*, 297. Irmeler, M.; Meyer, G. Z. *Anorg. Allg. Chem.* **1990**, *587*, 197.

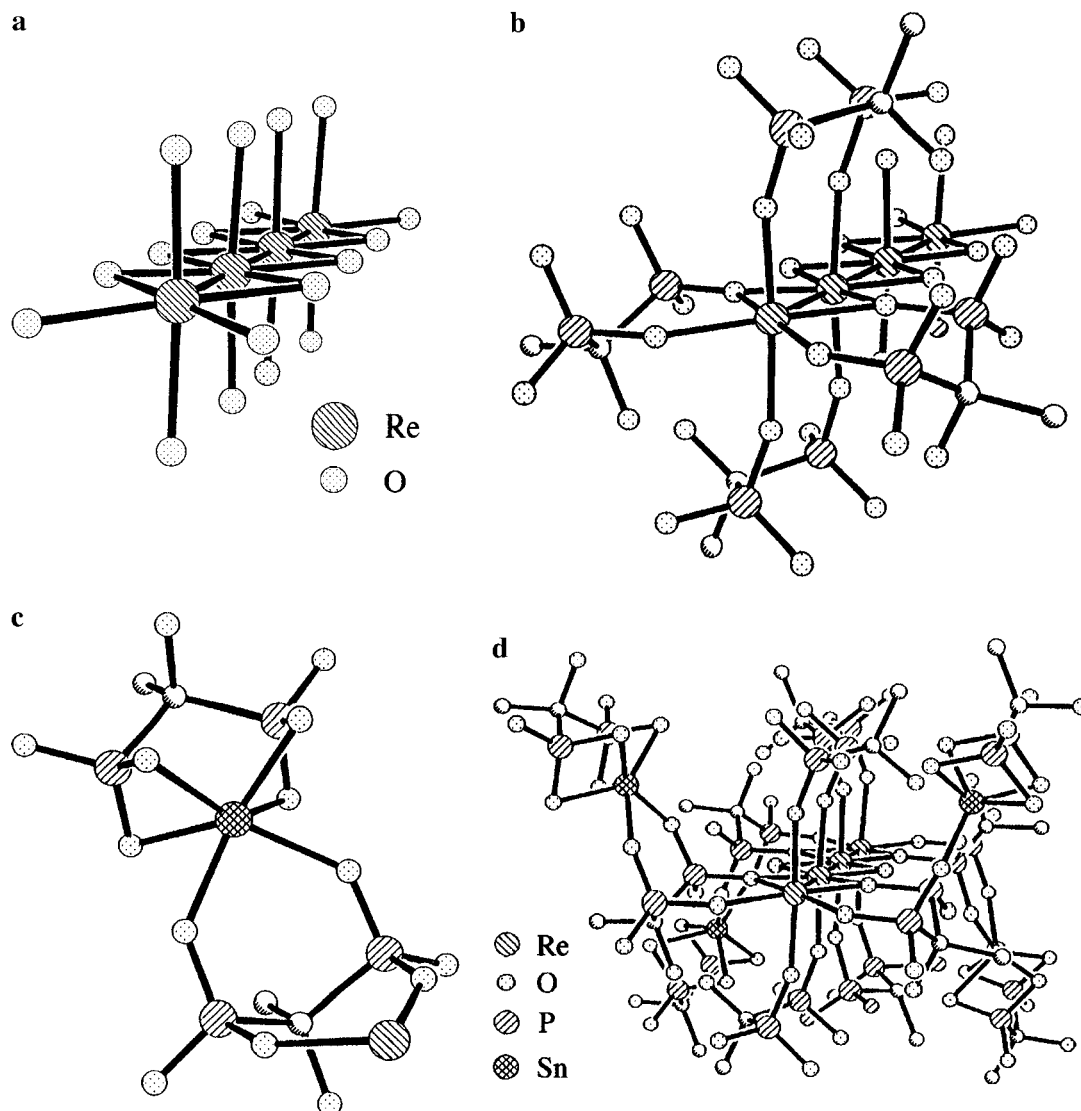


**Figure 7.** A possible structure for (H-Sn) ReHEDP. (a) The oxygen and rhenium framework. (b) Attachment of four HEDP ligands to the framework in a. (c) A tin atom tetracoordinated by one HEDP ligand. (d) Attachment of the remaining four HEDP ligands to the rhenium-oxygen framework in b and attachment of four SnHEDP units as shown in c to the exposed HEDP ligands.

All the other considerations are similar to those for (H-Sn) ReHEDP. However, it should be noted that, although the first shell coordination by oxygen remains six-fold, the geometry about rhenium is no longer octahedral.

Note also that this model has only eight HEDP ligands for three rhenium atoms. Its empirical formula, given a one to one rhenium to tin ratio, is  $[\text{Sn}_3\text{Re}_3(\text{HEDP})_8]^{n-}$ , where  $n$  depends on the extent of ionization of HEDP and the oxidation states of rhenium and tin. For this model there would be a P:Re atomic ratio of 5.33 in moderate agreement with the analytical value of 5.77.

**(Clin) ReHEDP.** Here the evidence supports even more complex behavior. The Re-Re fits of the EXAFS indicate both short and long Re-Re bonds and the two-shell Re-O fit indicates more long (four bridging distances of 2.07 Å) and fewer short (two terminal distances of 1.98 Å), indicating a cyclic structure. It appears that the clinical mixture is quite complex and probably is composed of structures found both in the (L-Sn) ReHEDP and (H-Sn) ReHEDP preparations.

When considering the formation of polymeric species such as those suggested here, one must be cautious whether species which form at high concentrations of metal ion will also be found when the preparations are more dilute. It is important to note, however, that the (Clin) ReHEDP, which appears to show

evidence of both trimer and tetramer formation, is less than 10-fold more concentrated than that used in the actual preparations undergoing clinical trials. As opposed to the bone-imaging, technetium analogues which are formed utilizing generator-produced  $^{99\text{m}}\text{Tc}$  at concentrations sometimes as low as  $10^{-9}$  M, the  $^{186}\text{Re}$  is a reactor product from neutron irradiation of enriched  $^{185}\text{rhenium}$  foil starting material. Between 1 and 10% of the target foil is converted to  $^{186}\text{Re}$ . The target is dissolved in acid, and enough material is used to achieve the desired rather high specific activity to irradiate the metastatic tumor. Thus the total rhenium concentrations used in preparing the actual clinical material approach millimolar.

**Comparison to the Crystal Structure of TcMDP.** The simplest of the diphosphonate family of ligands is methylenediphosphonate wherein the central carbon atom contains two hydrogen atom substituents rather than the methyl and hydroxyl substituents of HEDP. We published the crystal structure of a material which we represented as  $\{[\text{Li}(\text{H}_2\text{O})_3][\text{Tc}^{\text{IV}}(\text{OH})(\text{MDP})] \cdot \frac{1}{3}\text{H}_2\text{O}\}_n$ .<sup>33</sup> That material was synthesized by the substitution reaction of MDP on  $[\text{Tc}^{\text{IV}}\text{Br}_6]^{2-}$ . There are no short (bonding) Tc-Tc interactions, and the structure was described

(33) Libson, K.; Deutsch, E.; Barnett, B. L. *J. Am. Chem. Soc.*, **1980**, *102*, 2476.



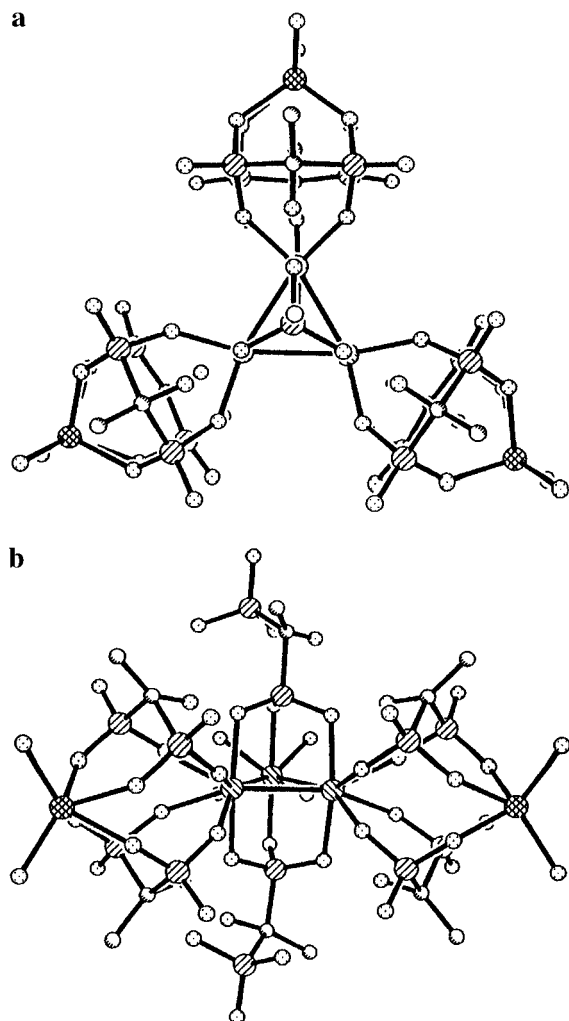


**Figure 8.** A possible structure for (L-Sn) ReHEDP. (a) A view along the three-fold axis of the cluster. The lower capping ligand is not shown and the upper HEDP capping ligand only shows the three oxygen atoms, one phosphorus atom, and the methylene carbon. (b) A view perpendicular to the three-fold axis. The back rhenium atom is only attached to four diphosphonate oxygen atoms without the rest of the ligand and its attached tin structure to simplify the view.

as an infinite polymer with technetium centers bridged by diphosphonate ligands. The space group of the crystal was  $R\bar{3}(\text{bar})$  with 18 formula units in the unit cell. The complex symmetry led us to overlook another structural aspect of the crystal which is indicated in Figure 9. As is obvious from the figure there is a basic hexagonal, cyclic arrangement of six technetium atoms bridged by six MDP ligands.

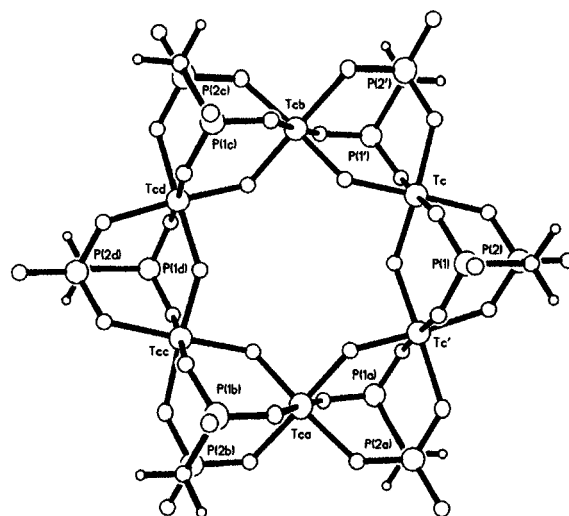


**Figure 9.** The structure of the cyclic hexamer found in the crystal structure of TcMDP.

Although the MDP complex is oligomeric, with similar bridging to that we have postulated for the various ReHEDP species, it is distinct in that there are no technetium—technetium bonds. Of course, (Subs) ReHEDP, which was also made by a substitution route, also has no Re—Re bonds, but it is unique as we have postulated it in having a discrete monomeric structure. That may well result from the use of absolute ethanol to retard the ionization of  $\text{H}_4\text{HEDP}$  so that only the  $[\text{H}_2\text{HEDP}]^{2-}$  dianion is present during the synthesis. The general features of the diphosphonate ligands seem to be that given a medium which supports their ionization to a tetraanion, such as  $[\text{HEDP}]^{4-}$ , the diphosphonate will become tetracoordinate and bridge metal centers to form polymeric materials. In the lower oxidation states of rhenium which are reached by the use of large excesses of the stannous reducing agent there is an additional driving force to polymerization, and delicate balances apparently exist between various polymers, such as the linear tetramer or the triangular cluster.

**Acknowledgment.** R.C.E. thanks Mallinckrodt Medical for support. We thank Dr. Douglas Ho for pointing out the cyclic hexamer unit in the crystal structure of TcMDP. EXAFS measurements were performed at the Stanford Synchrotron Radiation Laboratories which are operated by DOE and also supported by NIH and at the Cornell High Energy Synchrotron Source which is operated by the NSF. We thank Dr. Britt Hedman of SSRL for measuring the EXAFS of rhenium metal for us.

IC960980H